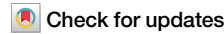




# Land conversion to energy crops for sustainable aviation fuel production reduces greenhouse gas emissions in the United States



Weiwei Wang<sup>1</sup>, Elena Blanc-Betes<sup>1</sup>, Madhu Khanna<sup>1,2,3</sup>, Chongya Jiang<sup>2</sup>, Kaiyu Guan<sup>1,2,4</sup>, Jeremy S. Guest<sup>1,2,5,6</sup>, John L. Field<sup>7,8</sup> & Evan H. DeLucia<sup>2,9</sup>

Energy crops will be critical for scaling up production of Sustainable Aviation Fuel in the United States and reducing greenhouse gas emissions. Here we examine the economic incentives for the extent and type of land conversion needed to scale up fuel production from a mix of cellulosic feedstocks and quantify its greenhouse gas intensity. We show that even with the availability of marginal non-cropland, there will be incentives for converting cropland to produce energy crops as the price of sustainable aviation fuel increases. But contrary to expectations, we find that scaling up fuel production by converting more cropland and more non-cropland from existing uses to energy crops lowers its net greenhouse gas intensity, due to high soil carbon sequestration rate of energy crops, even after considering land use change emissions. The potential savings in emissions are larger than the foregone soil carbon accumulation benefits from keeping that land in current uses.

There is growing policy support for reducing greenhouse gas (GHG) emissions from the aviation sector by inducing the production of sustainable aviation fuel (SAF) that is at least 50% less carbon-intensive than petroleum jet in the United States (U.S.)<sup>1</sup>. The SAF Grand Challenge, announced in 2021, aims to scale up domestic production of SAF to replace 100% of aviation fuel (about 35 billion gallons) by 2050. The U.S. Department of Energy Roadmap for SAF notes that these 2050 SAF goals cannot be reached without the use of biomass feedstocks, such as corn stover and dedicated energy crops<sup>1</sup>.

The US has the potential to produce a wide range of high-yielding energy crops, as well as crop residues from corn and wheat<sup>2</sup>. The per-unit cost of SAF and GHG intensity of SAF (GHG emissions per mega-joule of SAF) will differ with the feedstocks used<sup>3–5</sup>. There is also considerable spatial heterogeneity in yield and soil carbon sequestration rates for each of these feedstocks across the rainfed region of the U.S., which will affect the cost and GHG intensity of SAF with a feedstock across locations. Thus, the supply of

SAF at various prices and the GHG savings with SAF relative to petroleum jet will depend on the mix of feedstocks incentivized across locations and the availability of suitable land, which will affect the amount that can be produced. Crop residues provide a lower-cost feedstock for SAF but have relatively low yield and higher GHG intensity than energy crops because they lead to loss of soil carbon instead of soil carbon sequestration like energy crops (see Supplementary Information (SI) Section 2). Energy crops are high-yielding and have high soil carbon sequestration potential, but they are costly to produce, and their production raises concerns about inducing diversion of land from existing uses.

Energy crops have the potential to be produced on “marginal land”<sup>6</sup>, and Khanna et al.<sup>7</sup> show that economically marginal land (defined as land that is idle and would earn close to zero returns from crop production) would have economic incentives to convert to energy crops because its opportunity cost of conversion (or foregone returns from crop production) is low. However, the production of energy crops may not be limited to

<sup>1</sup>School of Business, Nanjing University of Information Science and Technology, Nanjing, China. <sup>2</sup>DOE Center for Advanced Bioenergy and Bioproducts Innovation (CABBI), University of Illinois Urbana–Champaign, Urbana, IL, USA. <sup>3</sup>Department of Agricultural and Consumer Economics, University of Illinois Urbana–Champaign, Urbana, IL, USA. <sup>4</sup>Department of Natural Resources and Environmental Sciences, University of Illinois Urbana–Champaign, Urbana, IL, USA.

<sup>5</sup>Department of Civil and Environmental Engineering, University of Illinois Urbana–Champaign, Urbana, IL, USA. <sup>6</sup>The Grainger College of Engineering, University of Illinois Urbana–Champaign, Urbana, IL, USA. <sup>7</sup>Environmental Sciences Division, Oak Ridge National Laboratory, Oak Ridge, TN, USA. <sup>8</sup>DOE Center for Bioenergy Innovation (CBI), Oak Ridge National Laboratory, Oak Ridge, TN, USA. <sup>9</sup>Department of Plant Biology, University of Illinois Urbana–Champaign, Urbana, IL, USA.

e-mail: [khanna1@illinois.edu](mailto:khanna1@illinois.edu)

marginal land because cropland can also have an economic incentive to convert to energy crops if the biomass price is high. Other non-cropland under grass or pasture may similarly have an economic incentive to produce energy crops.

Since different types of land and locations vary in their suitability, yields of energy crops, and costs of producing energy crops, the availability of various types of land for feedstock production will affect the mix of feedstocks and the location of their production. With heterogeneity in yield per unit land across feedstocks and locations, this in turn will affect the land requirement of various aggregate levels of SAF production, the extent of diversion of cropland for energy crops production, and consequences for food/feed crop production and food crop prices.

The mix of feedstocks and the land requirements for their production also have implications for the GHG intensity of SAF. The production of energy crops on cropland and non-cropland will directly affect carbon stocks on that land<sup>8</sup>. Furthermore, the diversion of cropland to energy crops can raise food crop prices and indirectly induce the conversion of non-cropland to food crop production. Both the direct and indirect causes of land use change, referred to as induced land use change (ILUC), can lead to changes in carbon stocks in the land and affect the overall GHG intensity of SAF.

Existing research has focused on analyzing the breakeven prices, carbon intensity, and land use requirements of individual feedstocks for SAF. Specifically, Fan et al.<sup>9</sup> conducted spatially varying techno-economic and life-cycle analysis to compare the spatially varying breakeven price of SAF and GHG intensity of miscanthus, switchgrass, sorghum, and corn stover, across the rainfed US. Gautam et al.<sup>10</sup> examine the amount of cropland that could be converted to miscanthus, sorghum, and switchgrass at a given price of soil carbon sequestration and jet fuel; they consider the potential to produce these feedstocks one at a time and do not examine their competition for land or the competition with food crops. Both these studies incorporate the direct soil carbon effects due to feedstock production, but have not analyzed their potential to be grown on non-cropland and the GHG intensity implications of various levels of SAF production. Global partial equilibrium models (GLOBIOM<sup>4,11,12</sup>) and general equilibrium economic models (such as GTAP-Bio<sup>5,13</sup>) have analyzed the GHG intensity of specific biofuel feedstock pathways for SAF one at a time. The US Department of Energy's Billion-ton Report<sup>2,14</sup> has examined the supply of biomass from a variety of different cellulosic feedstocks at various biomass prices.

None of these studies has analyzed the economically optimal mix of feedstocks for various levels of aggregate supply of SAF and the implications of varying constraints of availability of land on which they can be produced for this mix of feedstocks. Existing research has also not quantified the aggregate impacts of scaling up SAF production on GHG emissions and land use change, and the extent to which this will vary with land availability constraints.

The goal of this study is to fill these research gaps by undertaking a comprehensive analysis of the economic and GHG implications of biomass-based SAF production in the US. There exist several different pathways and feedstocks for SAF production. These include the Hydro-processed Esters and Fatty Acids (HEFA) pathway for converting oils and fats to SAF and the Fischer-Tropsch (FT) method for converting cellulosic feedstocks to biomass-based SAF. Our analysis focuses on the Alcohol-to-Jet Synthetic Paraffinic Kerosene (ATJ-SPK) pathway, which has relatively lower breakeven costs than FT and is not constrained by feedstock availability like HEFA<sup>15</sup>. We examine the economically optimal supply of biomass-based ATJ-SPK, from a wide range of agricultural feedstocks, under alternative scenarios, and quantify the GHG emissions intensity of various levels of supply of ATJ-SAF (defined to include the life-cycle emissions from feedstock production and conversion to SAF and the ILUC-related changes in soil carbon stocks). The life-cycle emissions intensity includes the emissions of producing the feedstock, conversion to ethanol, and upgrading ethanol to ATJ-SPK; no emission credits were applied to cogenerated gasoline- and diesel-range products

(as in ref. 9). The ILUC estimates are those within the US and do not consider international land use change.

We undertake this analysis by integrating the DayCent, a biogeochemical model of yield and GHG balance<sup>8</sup> with BEPAM, a partial equilibrium, recursive-dynamic, open economy optimization model<sup>16,17</sup>, and BioSTEAM, a feedstock-specific process engineering model of biorefineries<sup>18,19</sup> (see SI Fig. S1 and BEPAM model validation in SI Table S1 and Fig. S2; DayCent model validation in SI Figs. S3–S5). This modeling framework incorporates spatial heterogeneity in yields, costs, soil carbon sequestration rates, and land availability for a wide range of food/feed crops and biomass sources at a Crop Reporting District (CRD). The biomass sources include energy crops (miscanthus, switchgrass, energy sorghum, energy cane, short rotation woody crops (poplar and willow)), as well as crop residues from corn and wheat. The model considers competing demands for cropland and non-cropland for projected food, feed, and feedstock production and determines the welfare-maximizing allocation of land to a wide range of food and energy crops subject to technology, material balance, and land availability constraints. It determines land competition and allocation among alternative uses depending on the net present value of returns to each use. In addition to available cropland, we consider various types of non-cropland that can be converted to crop production, including economically marginal land, as well as grasslands in the US (SI Table S2).

Assessing the availability of economically marginal land is challenging, and Jiang et al.<sup>20</sup> use a history of satellite data on land use change to identify 4.3 million hectares of economically marginal land with confidence in the US; of this, 1.7 million hectares is idle and in the rainfed region that is suitable for energy crop production. There is a relatively larger amount of idle land that can be classified as economically marginal with uncertainty in the rainfed region (16.9 million hectares) (details in SI, Section 1; SI Fig. S6). We construct three scenarios of land area that can be potentially converted to crop (food crop and energy crop) production based on Jiang et al.<sup>20</sup>. These are implemented in BEPAM as land availability constraints, defined at the CRD level (see “Methods” section, SI Fig. S1). In each of these three scenarios, we analyze the incentives for the available land to produce a range of biomass feedstocks under a wide range of biomass prices. These scenarios are motivated by the potential for concerns about ILUC driving policy restrictions on the types of land that can grow energy crops (similar to the restrictions placed by the Renewable Fuel Standard on only using land brought into cultivation before 2007 for producing feedstocks for renewable fuel<sup>21</sup>). Concerns about expanding cropland and potential for loss of ecosystem services and stored soil carbon stocks may limit energy crops to cropland and “marginal” land with certainty. On the other hand, the desire to ease effects on food crop prices may lead to a willingness to allow conversion of non-cropland (marginal land with uncertainty and grasslands and pastureland) to energy crops. We examine the implications of these land availability scenarios for the supply of SAF at various prices and for food crop prices.

Since there are varying estimates of the carbon stocks that can be released due to land use change, referred to here as emissions factors (EFs)<sup>22–27</sup>, we consider three different model-based estimates of these ILUC-related carbon emissions in computing the overall GHG savings due to SAF production with each land availability and biomass price scenario<sup>13,28–30</sup>. We compare the GHG emissions intensity of SAF with that of the energy-equivalent level of petroleum jet to determine the potential GHG savings with the displacement of petroleum jet. We compare these savings in GHG emissions (difference between the GHG intensity of petroleum jet and SAF) with the foregone opportunities for nature-based carbon sequestration that would have occurred if that land were instead maintained/restored as grasslands<sup>31</sup>.

Our analysis makes several scientific contributions. By linking an economic model with a biogeochemical and process engineering model, our analysis shows that assuming that energy crops would be produced only on cropland<sup>10</sup>, or only on marginal land<sup>6,32</sup> will lead to underestimation of the economically viable potential to produce SAF from cellulosic feedstocks in the rainfed region of the US. Restricting energy crop production to cropland

only, limits the potential of SAF production to 83 B l (24 billion gallons) with a carbon intensity of  $23 \text{ gCO}_2\text{e MJ}^{-1}$ . Allowing non-cropland conversion for energy crop production could allow the US to meet the SAF Grand Challenge with cellulosic feedstocks and lower carbon intensity of  $15.5 \text{ gCO}_2\text{e MJ}^{-1}$ . This leads to a counter-intuitive finding that the GHG intensity of SAF decreases as more cropland and non-cropland is allowed to be converted to energy crop production, even after we account for land use change emissions. This is due to the high carbon sequestration potential of energy crops, which more than offsets the initial reduction in carbon stocks due to conversion of non-cropland to energy crop production. Our analysis also shows the implications of meeting the SAF Grand Challenge for food crop prices; we find that it would require converting 29 million hectares (12%) of cropland and non-cropland (about half of which would be cropland) to energy crops and raise the food crop price index by 18%. Our analysis highlights the choices we confront, including land use change, crop price increase, and GHG intensity reduction, in promoting SAF for decarbonizing the aviation sector and informs policy choices for SAF production from cellulosic feedstocks.

## Results

### Economically optimal supply of SAF

The total amount of cellulosic feedstock and SAF that was economically optimal to produce varied as biomass prices increased from  $\$40 \text{ Mg}^{-1}$  to  $\$140 \text{ Mg}^{-1}$  and as the flexibility for non-cropland to convert to crop production increased across the three scenarios of non-cropland availability (Fig. 1A–C and SI Table S3). Biomass production was economically viable at a minimum biomass price of  $\$40 \text{ Mg}^{-1}$ , with a maximum of 480 million metric tons (M Mg) of biomass (measured in dry tons with zero moisture) being produced when the price was as high as  $\$140 \text{ Mg}^{-1}$  in scenario (I) (CL + MLC) with cropland and least marginal land availability (CL + MLC). In scenarios (II) and (III) (CL + MLC + U and CL + MLC + U + G) with moderate and high availability of land for bioenergy crop production, total biomass supply increased to 628 M Mg and 900 M Mg (about one billion US tons), respectively, at a price of  $\$140 \text{ Mg}^{-1}$ .

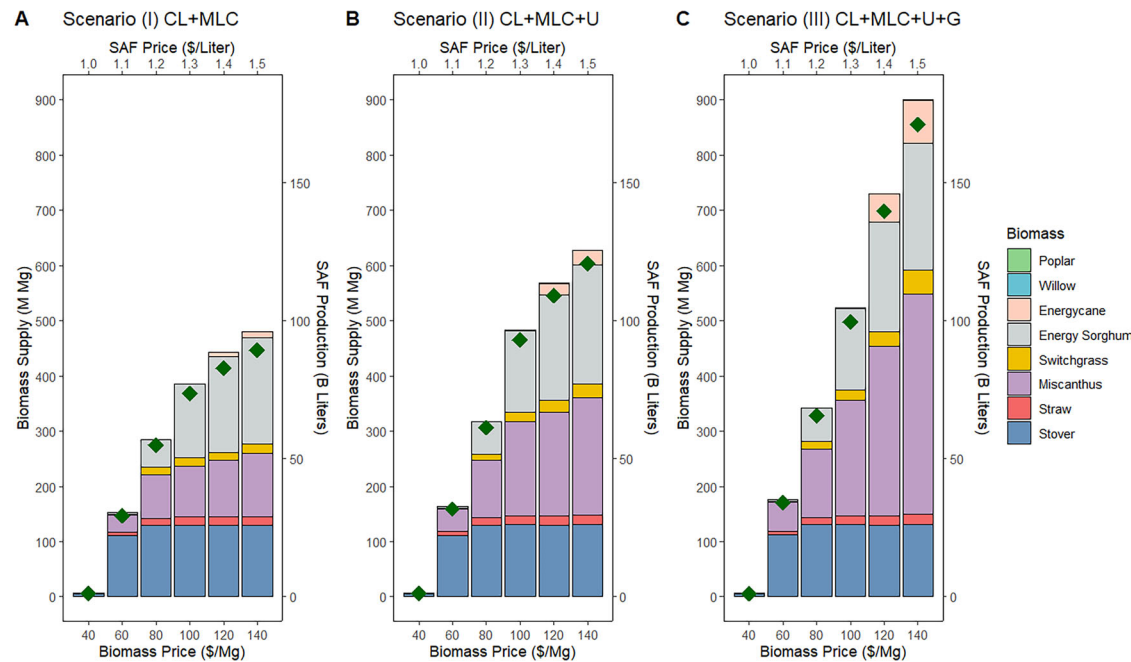


**Fig. 1 | Biomass supply under alternative price incentives and marginal land availability scenarios in 2030.** A Biomass supply curve under Scenario (I) CL + MLC. B Biomass supply curve under Scenario (II) CL + MLC + U. C Biomass supply curve under Scenario (III) CL + MLC + U + G. CL + MLC cropland and marginal land with confidence and uncertainty, CL + MLC + U + G cropland and marginal land with confidence and uncertainty and permanent grasslands. The bottom X-axis denotes the farm-gate price of biomass, and the top X-axis denotes the price of SAF production. Stacked bars indicate the biomass supply by various feedstock (left Y-axis). Green diamonds indicate the total SAF production (right Y-axis).

The biomass prices analyzed above implied SAF prices ranging from  $\$1.1 \text{ l}^{-1}$  to  $\$1.5 \text{ l}^{-1}$  (in 2016 dollars) to cover the cost of feedstock, transportation cost of feedstock, production cost of cellulosic ethanol (net of co-product electricity credit), and the cost of conversion to ATJ-SPK (SAF). SAF production at these prices ranged from 29 to 171 B l (8–45 B gallons) across the three land availability scenarios (Fig. 1). As the availability of low-cost land for production of energy crops increased, the amount of SAF that could be produced at a given price per liter of SAF increased (see SI Fig. S7). At  $\$1.4 \text{ l}^{-1}$ , the amount of SAF production ranged from 83 to 140 B l (22–37 B gallons); the upper end of this range of SAF production could displace 100% of the anticipated petroleum jet consumption in 2050. However, the minimum refinery-gate price of SAF of  $\$1.4 \text{ l}^{-1}$  ( $\$5.3 \text{ gallon}^{-1}$ ) is several-fold higher than the price of conventional jet fuel of  $\$0.34 \text{ l}^{-1}$  ( $\$1.3 \text{ gallon}^{-1}$ ) in 2016 dollars, and about twice as high as subsequent prices that rose to  $\$0.8 \text{ l}^{-1}$  ( $\$3 \text{ gallon}^{-1}$ ) in 2022. The gap in the price of SAF and the price of jet fuel of  $\$0.33$ – $\$0.46 \text{ l}^{-1}$  is substantially larger than the SAF tax credit that is currently being offered in the US<sup>1</sup>.

### Economically optimal mix and location of cellulosic feedstock production

The mix of feedstocks produced varied with the price of biomass and the availability of marginal land and grassland. Corn stover and wheat straw were the lowest cost sources of biomass and became viable at biomass prices between  $\$40$  and  $\$60 \text{ Mg}^{-1}$ . As biomass price increased, it created incentives for increasing the area under continuous corn and no-till (which allows a larger share of residue to be harvested) and reducing the area under corn-soybean rotation and the share of land under conventional tillage.

As biomass price increased and non-cropland availability increased, the share of two high-yielding but more costly feedstocks, miscanthus and energy sorghum, increased across all scenarios (Fig. 1 and SI Table S3). Higher biomass price made it economically viable to convert cropland to these energy crops. The share of other energy crops, such as willow and poplar, was positive but small because of their low yields and suitability for production in limited regions in the US.

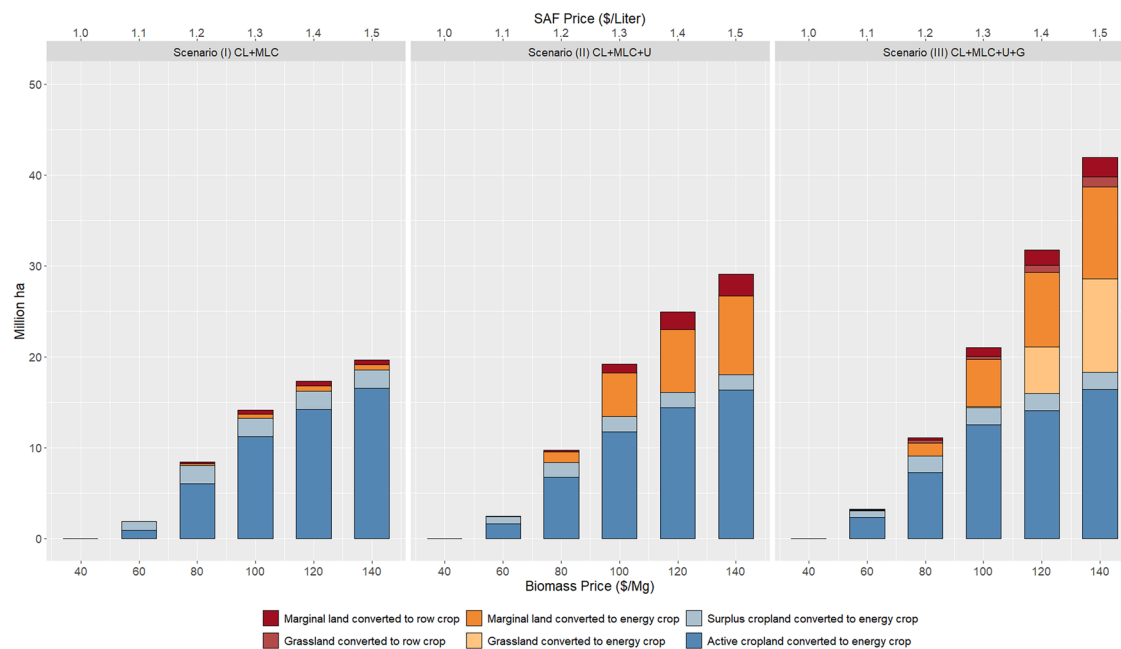


**Fig. 2 | Land use change under alternative price incentives and marginal land availability scenarios in 2030.** The value under each biomass price scenario is the net land use change relative to the zero biomass price. CL + MLC cropland and

marginal land with confidence, CL + MLC + U cropland and marginal land with confidence and uncertainty, CL + MLC + U + G cropland and marginal land with confidence and uncertainty and permanent grasslands.

The optimal locations for producing miscanthus, switchgrass, energy sorghum, and energy cane varied across the rainfed region of the US (see SI Fig. S8) due to differences in their yields, costs of production, and the opportunity cost of converting land for their production. Miscanthus production was economically viable largely in the Midwest and Atlantic states, while switchgrass was economically viable in the southern states. Energy cane production was confined to the Gulf states, while energy sorghum production was dispersed throughout the region.

#### Land-use change effects of SAF production

The type and amount of land used for cellulosic feedstock production varied with biomass price and the assumptions about land availability in the different scenarios, as shown in Fig. 2 and SI Table S4. In Scenario (I) (CL + MLC), energy crop production occurred mainly on cropland, followed by cropland that would become surplus in the future (if biomass price had remained at zero) and a small amount of marginal land. The maximum amount of SAF production would be limited to 91 B1 (24 B gallons), of which 61 B1 (16 B gallons) would be from energy crops and the rest from crop residues and require about 19 M hectares of land that was largely cropland. In scenario (II) (CL + MLC + U) with greater availability of marginal land for energy crops, the same amount of SAF could be produced with less diversion of cropland and greater conversion of marginal land to energy crops. The total amount of SAF that could now be produced is 120 B1 (32 B gallons) and would require converting 27 M ha to energy crops, of which about 9 M ha would be marginal land.

In Scenario (III) (CL + MLC + U + G) with the potential for a large amount of grassland to convert to crops, the amount of SAF production can increase to 171 B1 (45 B gallons) at a biomass price of  $140 \text{ Mg}^{-1}$ . The production of 140 B1 (37 B gallons) of SAF will require 39 M ha of land dedicated to energy crops, of which about 53% would be from non-cropland (SI Fig. S9 and Table S4). Despite the availability of large amounts of non-cropland in Scenario (III), cropland will be converted to produce energy crops, because much of the non-cropland is in the Great Plains and west of it (as shown in SI Fig. S6), where yields of energy crops are low and land is not rainfed and the cost of biomass production is higher on non-cropland than on cropland.

Production of energy crops will induce some spatial changes in food crop production and grazing land available for cattle. We find that in Scenario (III) with 37 B gallons of SAF production, there will be a loss of 11.7 million hectares of crop acreage in the rainfed region, and a 0.4 million hectare increase in irrigated acreage in states like Texas, Colorado, and California (SI Fig. S10). The conversion of non-cropland to energy crops reduced the availability of grazing land in some states (e.g., Arkansas, Texas, and Kentucky) and increased it in other states, such as Kansas, Oklahoma, Nebraska, and Montana. Overall, however, there was only a marginal effect on the number of cattle and the quantity of beef production and its price.

#### Effect of SAF production on food crop prices

As biomass prices increased, more cropland would be diverted from food/feed crop production for energy crops. We find that production of the major crops included in the economic model, such as soybeans, wheat, and sorghum, would decline by more than 15% in the case with a biomass price of  $140 \text{ Mg}^{-1}$  relative to the case with a biomass price of zero (SI Fig. S11A). This will also result in a substantial (15–25%) reduction in the exports of these crops (SI Fig. S11B). The reduction in crop production and exports will lead to an increase in crop prices (SI Fig. S12). We computed the Laspeyres Price Index for three major food crops, corn, soybeans, and wheat, at various levels of SAF production in 2030. As SAF production increased beyond 76 B1 (20 B gallons), this index increased by 15–30%; the extent of the increase was negatively related to the availability of non-cropland for conversion to crop production. The reduction in crop production and exports and the increase in food crop prices for a given level of SAF production were largest in Scenario (I), in which total active cropland for corn and soybeans was reduced by up to 10% and converted to energy crops. In Scenario (III), with the highest availability of non-cropland, the increase in food crop prices would be smaller because there would be less pressure on the use of land for crop production; an 18% increase in the food crop price index would accompany 37 B gallons of SAF production in Scenario (III) and 20 B gallons of SAF production in Scenario (I). Soybean prices increase more than corn prices because the area under soybeans sees a greater reduction than the area under corn as biomass prices increase. This is because the demand for corn stover creates incentives to switch from corn-soybean rotation to continuous corn, and this reduces the acreage under corn less than that under

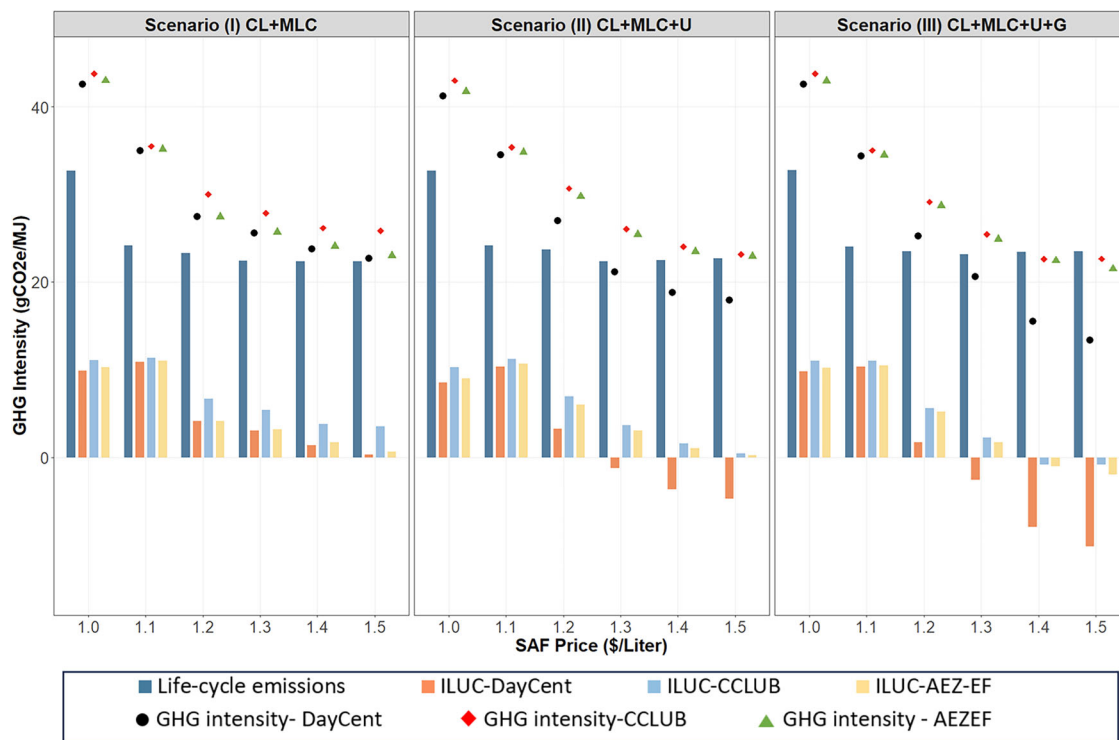


**Fig. 3 | GHG intensity of SAF production under different levels of SAF price.** Dark blue bars indicate GHG intensity with life-cycle emissions. Orange, light blue, and yellow bars represent ILUC GHG intensity associated with DayCent, CCLUB, and AEZ-EF, respectively. Black dots, red diamonds, and green triangles indicate total GHG intensity (life-cycle emissions + ILUC) associated with DayCent,

CCLUB, and AEZ-EF, respectively. CL + MLC cropland and marginal land with confidence, CL + MLC + U cropland and marginal land with confidence and uncertainty, CL + MLC + U + G cropland and marginal land with confidence and uncertainty and permanent grasslands.

soybeans. Wheat prices increase the most due to lower opportunity cost of converting wheat acreage to energy crops compared to acreage under corn and soybean in the Midwest and the negligible effects of demand for wheat straw on wheat acreage; however, at the highest SAF price simulated here, there is significant conversion of soybean acreage to energy crops and a higher increase in soybean price compared to wheat.

#### GHG implications

Our estimates of the GHG intensity of SAF show that it declines as the scale of aggregate biomass and SAF production increases and as land availability increases (Fig. 3). This is because, as SAF production scales up at higher SAF prices, the feedstock mix transitions from being largely crop residues to having a higher share of energy crops. The ILUC emissions, which include a reduction in soil carbon stocks due to conversion of non-cropland to crop production and due to harvesting of crop residues (see SI Fig. S5), as well as the gain in soil carbon stocks due to energy crop production, become increasingly small and even negative in Scenarios (II) and (III) as SAF production increases. ILUC emissions are positive at low biomass prices due to the loss in soil carbon stocks caused by the harvesting of even limited amounts of crop residue. These ILUC become overall negative at higher biomass prices as the share of energy crops in the biomass mix increases; the soil carbon sequestration due to energy crop production is much larger than the carbon emissions generated by the conversion of non-cropland due to their production. We estimated the ILUC emissions with three different EFs and found that the ILUC-related GHG intensity is generally highest with the CCLUB EF and lowest with the DayCent EF. The overall GHG intensity of SAF was estimated to range between 23 and 27 gCO<sub>2</sub>e MJ<sup>-1</sup> when there were 55–89 B (15–24 B gallons) of SAF with the least marginal land availability. The GHG intensity of SAF would be reduced to 13–25 gCO<sub>2</sub>e MJ<sup>-1</sup> when there were 65–171 B (17–45 B gallons) of production of SAF with the most generous marginal land availability. The reduction in GHG emissions intensity of SAF ranged from 75% with 24 B gallons of SAF production in

Scenario (I) to 83% with 37 B gallons of SAF production in Scenario (III) (SI Fig. S13). Despite differences in ILUC across different EF modeling approaches, the difference in estimates of net GHG intensity with the three EFs was small and within  $\pm 6\%$  on average (see Fig. 3). The two alternative ILUC EFs increased the GHG intensity of SAF from the reference range of 13–27 gCO<sub>2</sub>e MJ<sup>-1</sup> to 22–30 gCO<sub>2</sub>e MJ<sup>-1</sup> (see SI Table S5).

A higher level of SAF production and non-cropland availability also led to a greater amount of aggregate GHG savings (due to greater displacement of energy-equivalent jet fuel) relative to the scenario with zero biomass price (Fig. 4). At a given price of SAF, the GHG savings increased as the amount of non-cropland for conversion to energy crops increased. These savings ranged from about 207 M Mg CO<sub>2</sub>e with 24 B gallons of SAF in Scenario (I) to about 359 M Mg CO<sub>2</sub>e with 37 B gallons of SAF in Scenario (III); these represented 75% and 83% of emissions from the aviation sector with energy equivalent gallons of petroleum jet fuel consumption (SI Fig. S14 and Table S6). These savings remained substantial even after we considered the uncertainty in various modeling assumptions about crop yields, SAF production costs, and ILUC EFs. The overall potential for reduction in GHG emissions from the aviation sector would range from 163 to 261 M Mg CO<sub>2</sub>e with 24 B gallons of SAF in Scenario (I) to 295–444 M Mg CO<sub>2</sub>e with 37 B gallons of SAF in Scenario (III) (Fig. 4).

Although we found that SAF production resulted in GHG savings relative to petroleum jet, the change in soil carbon stock varied over time (SI Fig. S15A). The conversion of land to energy crops generated an initial soil carbon loss derived from soil disturbance during the conversion of non-cropland to cropland (carbon debt). This soil carbon debt was larger at higher biomass and SAF prices, and as land availability increased due to a higher share of energy crops. The carbon debt payback period decreased with larger biomass price and land availability because there was greater production of miscanthus in these scenarios, and miscanthus had a high rate of soil carbon sequestration. We found that the ILUC due to energy crop production led to a soil carbon debt that would take 5–7 years to pay back

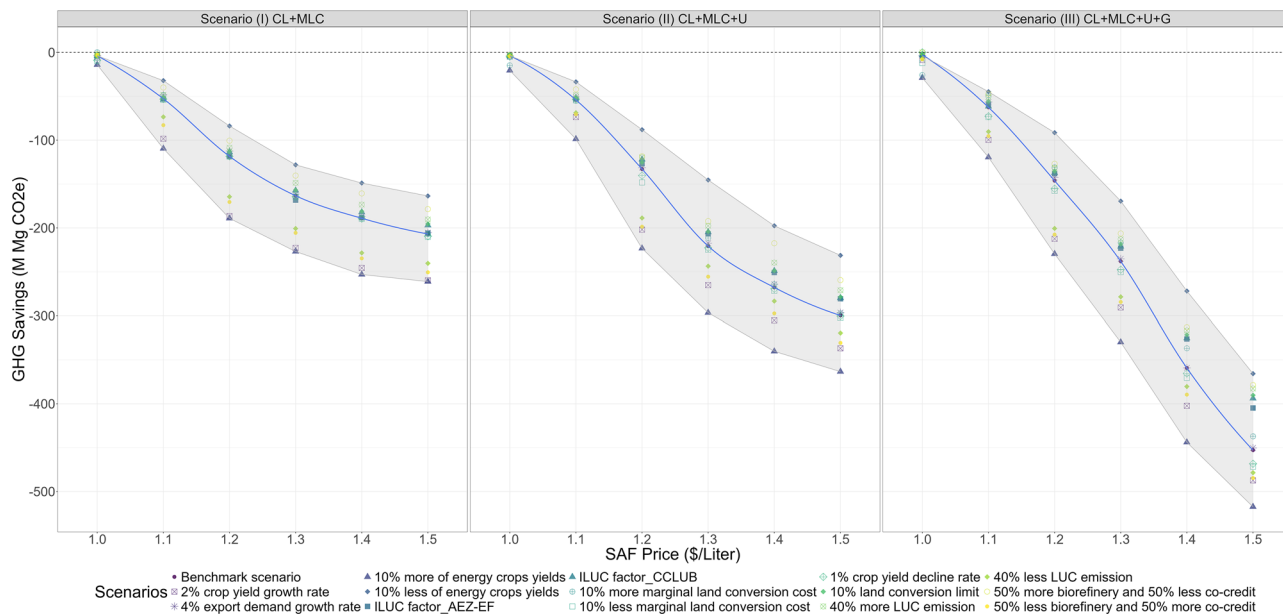


**Fig. 4 | Sensitivity analysis of GHG savings in 2030 under alternative scenarios.**

The blue lines show the GHG savings under the benchmark scenario, net of land use change emissions. Different markers represent GHG savings under different scenarios in the sensitivity analysis. The shaded areas indicate the range of resulting

GHG savings. CL + MLC cropland and marginal land with confidence, CL + MLC + U cropland and marginal land with confidence and uncertainty, CL + MLC + U + G cropland and marginal land with confidence and uncertainty and permanent grasslands.

through additional soil carbon sequestration by energy crops, with the shortest period occurring at the highest level of biomass price and land availability. The corresponding payback periods with CCLUB and AEZ-EF EFs were very close to those with the DayCent model. The 5–7 payback period of soil carbon debt was found to be robust to alternative assumptions of parameters analyzed in the sensitivity analysis.

We compared these savings with the foregone soil carbon sequestration that could have been achieved in the absence of biomass production (that is, with a biomass price of zero). The payback period required to compensate for the foregone soil carbon sequestration by energy crop production alone extended to 7–14 years across all scenarios; it was shortest in Scenario (I) with the lowest amount of forgone soil carbon sequestration and longest in Scenario (III). Corresponding payback periods for CCLUB and AEZ-EF were 5–12 years and 8–15 years, respectively, close to those with the DayCent model. These payback periods were significantly lower than the 90-year repayment period associated with producing corn grain ethanol on land under the Conservation Reserve Program<sup>33</sup>. Our findings are consistent with the results from a prior study that a 0–5 year payback period was achievable with biofuels supplied by miscanthus grown on grasslands at a global scale<sup>34</sup>.

However, this payback period would be reduced to less than 1 year when potential fossil fuel displacement benefits were considered, and was similar to all three LUC EFs (see SI Fig. S15B). After including the GHG savings due to the displacement of fossil fuels, we found that the GHG savings with SAF production were 20-fold larger than the savings obtained by restoring abandoned cropland and marginal land to grassland as in Scenario (I), and 8-fold larger than the level obtained by preserving the converted grasslands in Scenario (III).

## Discussion

Meeting the SAF Grand Challenge will require substantially expanding SAF production from 16 million gallons currently to more than 35 B gallons in the coming decades. With substantial shares of corn and soybeans already being used for biofuel, expansion of SAF production is expected to require going beyond food crops to cellulosic feedstocks. There are many choices of cellulosic feedstocks, including crop residues, perennial energy crops, and short rotation woody crops, and

considerable spatial heterogeneity in their yields, costs of production, and GHG intensity across the rainfed region. There is also a policy choice of the types of land, cropland, marginal land, and grasslands, which should be allowed to produce energy crops to meet the demand for SAF. Our analysis shows the trade-offs that scaling up of SAF production will pose for land use change, GHG intensity, and food crop prices. We find that as the amount of non-cropland available to produce SAF feedstocks was allowed to increase, the amount of cropland converted to energy crops decreased, and the impact on food crop prices decreased. Moreover, the GHG intensity of SAF also decreased because it would become economically viable to produce more energy crops, which would lead to an increase in soil carbon sequestration that was greater than the loss in soil carbon stocks due to land use change.

More specifically, 24–37 B gallons of SAF production would require converting about 8–12% of available cropland, marginal land, and non-cropland in the model to energy crops. The increase in SAF production would reduce food/feed crop production and exports and increase crop prices; the extent to which this is the case varies across crops. The impact on some crops, such as soybeans and wheat, for which the US is a large producer and exporter in the world market, could pose risks to food security within the US and internationally.

The effects of a given level of SAF production on food crop prices were negatively related to the availability of non-cropland; 24 B gallon of SAF production would be accompanied by 30% increase in crop price index if feedstock production is restricted to cropland and to 15% increase in crop price index if marginal land and grassland can be utilized for feedstock production and a 37 B gallon SAF production would be accompanied by a 18% increase in the food crop price index. Additionally, allowing 24 B gallons of SAF feedstock production to expand on grasslands would result in a lower GHG intensity of 20.6 gCO<sub>2</sub>e MJ<sup>-1</sup> compared to 22.7 gCO<sub>2</sub>e MJ<sup>-1</sup> with restricting it to cropland and marginal land with confidence only.

The production of SAF from crop residues alone would reduce GHG emissions intensity by 50% relative to the level with a biomass price of zero. With higher levels of land conversion to energy crop production, the GHG emissions intensity reduction with SAF production of 24–37 B gallons ranged from 75% to 83% relative to petroleum jet. We also find that conversion of marginal and grasslands to energy crops that displace fossil fuels

can lead to greater GHG savings than can be achieved by restoring and maintaining land as grasslands.

A key challenge to scaling up biomass-based SAF is its high cost relative to the price of petroleum jet. The SAF tax credit per unit of SAF currently being offered is insufficient to cover this price gap. Our analysis can be used to determine the tax credit (gap between the price of SAF and the price of petroleum jet per unit) that will be needed to incentivize various levels of biomass-based SAF production. It shows that the tax credit needed to induce a given volume of SAF will be lower as the land availability constraint is eased to include more marginal and non-cropland. Additionally, our analysis shows that given the numerous choices for feedstocks that differ in their carbon intensity, a tax credit per unit SAF that increases as the carbon intensity of SAF decreases will be more effective in inducing low-carbon SAF than a volumetric tax credit. The latter will incentivize the lowest cost feedstocks and not the feedstocks that have the lowest carbon intensity but relatively high cost of production.

There are several technical and infrastructural challenges to scaling up energy crop production, particularly on non-cropland, that were not considered in this analysis. Scaling up energy crop production will require planting material that could take several years to build. It may also require diverting non-cropland from other services such as hunting, open space, or wilderness, and this may make landowners reluctant to convert it to energy crops (Skevas et al.<sup>35</sup>); this could increase the opportunity cost of producing energy crops on this land and the biomass price needed to induce their production. Additionally, significant investment may be needed to create the roads and other infrastructure that will enable industrial-scale production of energy crops on land that had been abandoned from agriculture. The focus of this study is on analyzing the supply side of SAF production at the refinery gate and its land use change implications. We do not consider the transportation of SAF from biorefineries to the airports. Our analysis informs optimal location choices for feedstock production but leaves the biorefinery siting to future research.

Our analysis also assumed that landowners would choose the crop with the highest discounted value of returns over a time period. Risk-averse farmers will also consider the riskiness of income streams with conventional crops and energy crops. High upfront costs of establishment, time lags between planting and harvesting of perennial energy crops, and the need for long-term commitments to earn returns over the lifespan of the crop can raise the biomass price at which farmers would be willing to grow these crops<sup>36</sup>.

The biomass production and GHG savings obtained here at various biomass prices and land availability scenarios should, therefore, be an upper bound. Our analysis focused on the technical potential to displace petroleum jet and mitigate GHG emissions. The extent to which biomass-based SAF will displace jet fuel in the market will depend on market conditions and may be limited by changes in oil prices due to large-scale SAF production, which may lead to a rebound effect in domestic and global fuel markets.

The supply of SAF under various land availability constraints simulated here is determined under implicit assumptions about macroeconomic factors, such as growth in population, growth in Gross Domestic Product, and so on. These factors can affect demand for food crops and derived products over time, and the competition for cropland with SAF feedstocks. The framework developed here can be extended by specifying alternative scenarios of demand for food crops and derived products, induced by macro-economic drivers, and simulating their effects on the availability of cropland for SAF feedstock production and its implications for the supply of SAF.

While scale-up of SAF is essential for decarbonizing the aviation sector, its deployment should be carefully managed to avoid worsening energy security in a climate-disrupted world. A diversified portfolio of feedstock sources for SAF and a mix of alternative fuels in the aviation sector may be needed to increase resilience to extreme events and climate change.

Lastly, we do not consider the potential to produce forest biomass for bioenergy or the implications of biomass markets for the conversion of land between crops and forest. We refer readers to Valin et al.<sup>37</sup> and the Billion

Ton Study<sup>14</sup>, which find a small share of biomass (for bioenergy) that would be produced from forests in the EU and US, respectively; the latter also notes that much of the land use change from forest land is expected to be towards urban land rather than cropland. We leave further investigation of these issues for future research.

## Methods

### Alternative scenarios

We obtained biomass supply curves, over a wide range of biomass prices, and their GHG outcomes under three scenarios that differed in their definition of land assumed to be available for conversion to crop production (see SI Fig. S1). Specifically we considered three land availability scenarios: Scenario (I) assumed that cropland (CL) and economically marginal land with confidence (CL + MLC) can convert to crop production; Scenario (II) assumed that cropland and economically marginal land with confidence and with uncertainty (CL + MLC + U) can convert to crop production; Scenario (III) assumed that cropland, as well as marginal land with confidence and uncertainty and permanent grassland (CL + MLC + U + G) can convert to cropland (see SI Fig. S6 and Table S2 for detailed description of land types).

With each of the land availability scenarios, we simulated the economic incentives, with biomass prices ranging from zero to \$140 Mg<sup>-1</sup>, to produce a variety of energy crops and crop residues. We determined the type of land that will be converted to energy crops and their implications for land use change. In addition, in each of these scenarios, we also accounted for cropland that will become idle (surplus) over the 2016–2030 period in the absence of any biomass production (with a biomass price of zero) as growth in crop productivity outpaces demand for agricultural commodities. We allowed it to convert to energy crop production in scenarios with a positive price of biomass.

With each of the three land availability scenarios and biomass prices, we considered three alternative estimates of EFs. These are obtained from (i) DayCent Model simulations (DayCent-EF)<sup>8</sup> (ii) Carbon Calculator for Land Use and Land Management Change from Biofuels Production (CCLUB-EF) based on CENTURY model<sup>38</sup>, and (iii) Agro-ecological zone emission factor model (AEZ-EF)<sup>26,27,29</sup> (for more details see SI Section 5). The limitations and strengths of these models have been discussed in the existing literature<sup>22,26,27,39</sup>.

### Modeling the economic incentives for land allocation

The version of BEPAM (Biofuel and Environmental Policy Analysis Model) applied here models the agricultural sector and determines economically optimal land-use and feedstock mix at the US scale by maximizing the sum of agricultural sector consumers' and producers' surplus subject to various resource balances, land availability, and technological constraints under a range of biomass prices, from zero to \$140 Mg<sup>-1</sup> over the 2016–2030 period. The model endogenously determines optimal land use allocation for thirteen row crops and six energy crops on both cropland and non-cropland endogenously based on the biomass prices, availability of land, and the net returns to crop production. The model includes several sources of biomass, including herbaceous energy crops (miscanthus, switchgrass, energy sorghum, energy cane), short rotation woody crops (poplar and willow), and crop residues (corn stover and wheat straw). It also includes livestock production and various processed commodity markets. In the crop and livestock markets, primary crop and livestock commodities are consumed either domestically or traded with the rest of the world. Domestic and export demand for each of the agricultural commodities is exogenously given. The model simulates food/feed crop, livestock, and biomass production, consumption, and prices that ensure market demand and supply are in equilibrium at various biomass prices.

The model was applied to simulate the land-use decisions for 304 CRDs by incorporating the spatially heterogeneous yields of different crops obtained from DayCent and returns to producing them, and land availability constraints. The DayCent model was applied to simulate yields and soil carbon sequestration with row crops (corn and soybeans), corn stover,

and energy crops on cropland and on marginal land. This integrated modeling framework endogenously determined annual future returns and costs of production of each type of crop on each type of land (e.g., cropland, marginal land) at the CRD level. The costs of inputs and field operations were calculated at the CRD level for each crop and land type. The opportunity cost of land for producing energy crops was endogenously determined by the shadow price of the land constraint in the model.

Land allocation in BEPAM is determined by assuming that landowners use a 10-year rolling horizon to make decisions. Land is converted to alternative uses depending on the net present value of returns to alternative uses over the rolling horizon, including the cost of land conversion. The model is run for 10 years at a time and uses the first year's solution to update market conditions and then runs the model again for the next 10 years, and so on, with a rolling horizon. Specifically, the model first solves for the 2016–2025 period; we then take the first-year solution values, such as land allocation among different uses and crop prices as 'realized', move the horizon one year forward, and solve the new problem, and iterate until the problem is solved for year 2030 (the last simulation for the period 2030–2039).

Since our focus is on analyzing the incremental land use effects of cellulosic feedstock production at various biomass prices, we keep all other demands on land the same as in the zero biomass case. We assumed that production of first-generation biofuels is maintained at their level in 2016 across scenarios and over the simulation period. For simplicity, annual corn-based ethanol production is assumed to be at the maximum permitted level of 15 billion gallons, and the model does not consider exports of corn ethanol. Demands for other first-generation biofuels are exogenously fixed at 2016 levels following the EIA Outlook.

We used three-year (2014–2016) average prices, consumption, exports, and imports of crop and livestock commodities to calibrate the domestic demand, export demand, and import supply functions for all commodities. Domestic demands, export demands, and import supply curves were assumed to grow over time at exogenously specified rates based on the FAPRI 2010 U.S. and World Agricultural Outlook. In our model, we assumed the average annual shift rates presented in this outlook applied to the entire simulated period. More details of the BEPAM and DayCent model and their validation can be found in the SI (Sections 2 and 3; SI Figs. S2–S5 and Table S1).

BEPAM has several features that make it appropriate for the analysis in this paper. First, it has a high level of spatial heterogeneity, which enables a more detailed representation of agricultural activities at the CRD-level (for 304 CRDs in the US). This enables us to incorporate spatial heterogeneity in yields, carbon sequestration and costs of production of various cellulosic feedstocks at a finer scale relative to existing integrated models which are at an agro-ecological zone, sub-national or US water basin level (e.g., GTAP and GCAM-USA)<sup>29,40,41</sup> and to endogenously determine the mix of various energy crops that will be produced at various biomass prices and land availability scenarios. As our analysis shows, there is a significant difference in yields across feedstocks and the optimal location of feedstocks. Second, BEPAM enables us to develop an integrated framework with DayCent and BioSTEAM to include the spatially explicit yields and soil carbon sequestration with various feedstocks and to incorporate the techno-economic and life-cycle analysis for various biomass feedstocks and conversion processes at a feedstock-specific level. Third, it is a multi-period, recursive dynamic model, which makes it well-suited for studying perennial energy crops and updating the agricultural market conditions farmers face dynamically. The rolling horizon setting is more consistent with farmers' planning process than the traditional forward-looking models, which involve a single run of the model for the entire simulation period.

### Availability of non-cropland

We identified economically marginal land as land that is intermittently switching between crop and non-crop (see ref. 20). Estimates of economically marginal land availability in our modeling framework were

derived from the Cropland Data Layer (CDL) provided by the National Agricultural Statistics Service (NASS) using methods described in Jiang et al.<sup>20</sup> (see SI Section 1). We distinguished between land that can be classified as marginal with statistical confidence and marginal with uncertainty, as well as land that can be classified as permanent grassland and permanent cropland based on the analysis by Jiang et al.<sup>20</sup>. They found that the amount of land that could be classified as economically marginal with certainty in the rainfed region was small (1.7 million hectares) and that there was a substantial amount of land in the rainfed region that could only be classified as economically marginal with uncertainty (16.9 million hectares) in 2016. They also identified permanent grassland, which had been permanently in grass over the 2008–2015 period. Since we are unable to distinguish between grassland and pastureland from CDL data, both categories are included in the category defined as grassland. The availability and spatial distribution of non-cropland under each scenario are shown in SI Fig. S6.

### GHG emissions assessment

The GHG emission effects of SAF accounted for in this study included the following two components: (1) life-cycle GHG emissions (that occur aboveground and are also referred to as supply chain emissions) and include all emissions due to the harvesting of crop residues for biomass (including harvesting and replacement fertilizer application), planting of energy crops to their harvest (emissions from fertilizer, chemicals, fuels and machinery), transport to the refinery and conversion to SAF in the refinery. The process of conversion of biomass to (ATJ-SPK) SAF leads to the co-generation of electricity that displaces grid electricity and creates a co-product carbon credit that is subtracted from these life-cycle emissions, (2) induced land-use change related changes in soil-carbon stocks caused directly by the production of energy crops and removal of crop residues for biomass, including soil organic carbon, nitrous oxide and methane fluxes and changes in vegetation when energy crops are planted on non-cropland, as well as changes in soil carbon stocks caused indirectly by the change in crop and land prices induced by the conversion of cropland to energy crop production (see SI Section 2).

We assessed GHG savings from the aviation sector by comparing the sum of the life-cycle and ILUC emissions with SAF production with corresponding emissions from petroleum jet, assuming displacement on an energy-equivalent basis. We quantified the GHG emissions in 2030 from sources described above. We compared these emissions with the emissions from petroleum jet fuel on an energy-equivalent basis. This represents the technical GHG mitigation potential of cellulosic feedstocks since it does not consider any feedback effects on aviation fuel markets of large-scale displacement of jet fuel. The GHG emissions from converting cellulosic feedstocks to cellulosic ethanol in  $\text{gCO}_2\text{e MJ}^{-1}$  were measured based on the conversion coefficients of producing cellulosic ethanol from different feedstocks and carbon emission intensity as simulated by BioSTEAM. We assumed that cellulosic ethanol was converted to SAF via the ATJ-SPK pathway, and no emission credits were included for cogenerated gasoline- and diesel products. The emissions of upgrading ethanol to SAF were calculated based on the emission factor of producing jet from ethanol (21  $\text{gCO}_2\text{e MJ}^{-1}$  jet) reported by the GREET model. Emissions of converting ethanol to SAF were assumed to remain the same for all feedstock-based cellulosic ethanol.

We then compared the GHG savings with SAF obtained above to the foregone carbon sequestration on land that is converted to energy crop production instead of remaining or being restored to grasslands. We assessed this by including soil carbon sequestration that would have been obtained by (1) preserving grassland as unharvested; (2) restoring surplus cropland to grassland, and (3) restoring marginal land to grassland (instead of converting these lands to energy crops). Details of the methods for the computation of GHG savings and forgone carbon sequestration are presented in the SI Section 5. The average rates of annual soil carbon sequestration per hectare with various feedstocks are shown in SI Fig. S5.

## Data availability

The source data that support the findings of this study are openly available in a permanent repository on Illinois Data Bank ([https://doi.org/10.13012/B2IDB-7387487\\_V1](https://doi.org/10.13012/B2IDB-7387487_V1)). The marginal land data used in this study is available at: <https://cabbi.bio/datasets/assessing-marginal-land-availability-based-on-land-use-change-information-in-the-contiguous-united-states/>.

## Code availability

The DayCent model scripts and calibration files are available on the Illinois Data Bank ([https://doi.org/10.13012/B2IDB-7710407\\_V1](https://doi.org/10.13012/B2IDB-7710407_V1)). The BioSTEAM model is an open-source platform available at: <https://github.com/BioSTEAMDevelopmentGroup>. Emission factors model AEZ-EF (v52) is accessible at: [https://www.gtap.agecon.purdue.edu/resources/res\\_display.asp?RecordID=4346](https://www.gtap.agecon.purdue.edu/resources/res_display.asp?RecordID=4346). Information about the CCLUB model is available at: <https://publications.anl.gov/anlpubs/2025/05/193639.pdf>.

Received: 7 February 2025; Accepted: 14 October 2025;

Published online: 25 November 2025

## References

1. US Department of Energy. *SAF Grand Challenge Roadmap: Flight Plan for Sustainable Aviation Fuel* (US Department of Energy, 2022); <https://www.energy.gov/sites/default/files/2022-09/beto-saf-gc-roadmap-report-sept-2022.pdf>.
2. US Department of Energy. *2023 Billion-Ton Report: an Assessment of U.S. Renewable Carbon Resources* (US Department of Energy, 2024); [https://www.energy.gov/sites/default/files/2024-03/beto-2023-billion-ton-report\\_0.pdf](https://www.energy.gov/sites/default/files/2024-03/beto-2023-billion-ton-report_0.pdf).
3. International Civil Aviation Organization. *CORSIA Default Life Cycle Emissions Values for CORSIA Eligible Fuels* (ICAO, 2021); <https://www2023.icao.int/environmental-protection/CORSIA/Documents/ICAO%20document%2006%20-%20Default%20Life%20Cycle%20Emissions%20-%20March%202021.pdf>.
4. Prussi, M. et al. CORSIA: The first internationally adopted approach to calculate life-cycle GHG emissions for aviation fuels. *Renew. Sustain. Energy Rev.* **150**, 111398 (2021).
5. Zhao, X., Taheripour, F., Malina, R., Staples, M. D. & Tyner, W. E. Estimating induced land use change emissions for sustainable aviation biofuel pathways. *Sci. Total Environ.* **779**, 146238 (2021).
6. Gelfand, I. et al. Sustainable bioenergy production from marginal lands in the US Midwest. *Nature* **493**, 514–517 (2013).
7. Khanna, M. et al. Redefining marginal land for bioenergy crop production. *GCB Bioenergy* **13**, 1590–1609 (2021).
8. Blanc-Betts, E. et al. Climate vs energy security: quantifying the trade-offs of BECCS deployment and overcoming opportunity costs on set-aside land. *Environ. Sci. Technol.* **57**, 19732–19748 (2023).
9. Fan, X. et al. Spatially varying costs of GHG abatement with alternative cellulosic feedstocks for sustainable aviation fuels. *Environ. Sci. Technol.* **58**, 11352–11362 (2024).
10. Gautam, S., Baral, N. R., Mishra, U. & Scown, C. D. Impact of bioenergy feedstock carbon farming on sustainable aviation fuel viability in the United States. *Proc. Natl. Acad. Sci. USA* **120**, e2312667120 (2023).
11. Havlik, P. et al. Global land-use implications of first and second generation biofuel targets. *Energy Policy* **39**, 5690–5702 (2011).
12. Mosnier, A. et al. Alternative U.S. biofuel mandates and global GHG emissions: the role of land use change, crop management and yield growth. *Energy Policy* **57**, 602–614 (2013).
13. Taheripour, F. & Tyner, W. E. Induced land use emissions due to first and second generation biofuels and uncertainty in land use emission factors. *Econ. Res. Int.* **2013**, 1–12 (2013).
14. US Department of Energy. *2016 Billion-Ton Report, Volume 2: Environmental Sustainability Effects of Select Scenarios from Volume 1* (US Department of Energy, 2016); [https://www.energy.gov/sites/default/files/2017/02/f34/2016\\_billion\\_ton\\_report\\_volume\\_2\\_front\\_cover.pdf](https://www.energy.gov/sites/default/files/2017/02/f34/2016_billion_ton_report_volume_2_front_cover.pdf).
15. Okolie, J. A. et al. Multi-criteria decision analysis for the evaluation and screening of sustainable aviation fuel production pathways. *iScience* **26**, 106944 (2023).
16. Hudiburg, T. W. et al. Impacts of a 32-billion-gallon bioenergy landscape on land and fossil fuel use in the US. *Nat. Energy* **1**, 1–7 (2016).
17. Khanna, M., Wang, W., Hudiburg, T. W. & DeLucia, E. H. The social inefficiency of regulating indirect land use change due to biofuels. *Nat. Commun.* **8**, 15513 (2017).
18. Shi, R. & Guest, J. S. BioSTEAM-LCA: an integrated modeling framework for agile life cycle assessment of biorefineries under uncertainty. *ACS Sustain. Chem. Eng.* **8**, 18903–18914 (2020).
19. Cortes-Peña, Y., Kumar, D., Singh, V. & Guest, J. S. BioSTEAM: A Fast and Flexible Platform for the Design, Simulation, and Techno-Economic Analysis of Biorefineries under Uncertainty. *ACS Sustainable Chem. Eng.* **8**, 3302–3310 (2020).
20. Jiang, C., Guan, K., Khanna, M., Chen, L. & Peng, J. Assessing marginal land availability based on land use change information in the contiguous United States. *Environ. Sci. Technol.* <https://doi.org/10.1021/acs.est.1c02236> (2021).
21. EPA. What are the RFS2 Requirements for Renewable Fuel Producers to Track Soy Feedstocks? (EPA, 2024); <https://www.epa.gov/fuels-registration-reporting-and-compliance-help/what-are-rfs2-requirements-renewable-fuel>.
22. Scully, M. J., Norris, G. A., Alarcon Falconi, T. M. & MacIntosh, D. L. Carbon intensity of corn ethanol in the United States: state of the science. *Environ. Res. Lett.* **16**, 043001 (2021).
23. Chen, L. et al. Assessing the returns to land and greenhouse gas savings from producing energy crops on Conservation Reserve Program land. *Environ. Sci. Technol.* **55**, 1301–1309 (2021).
24. Qin, Z., Dunn, J. B., Kwon, H., Mueller, S. & Wander, M. M. Soil carbon sequestration and land use change associated with biofuel production: empirical evidence. *GCB Bioenerg.* **8**, 66–80 (2016).
25. Fargione, J. E. et al. Natural climate solutions for the United States. *Sci. Adv.* **4**, eaat1869 (2018).
26. Malins, C., Plevin, R. & Edwards, R. How robust are reductions in modeled estimates from GTAP-BIO of the indirect land use change induced by conventional biofuels?. *J. Clean. Prod.* **258**, 120716 (2020).
27. Taheripour, F., Mueller, S. & Kwon, H. Response to “How robust are reductions in modeled estimates from GTAP-BIO of the indirect land use change induced by conventional biofuels?”. *J. Clean. Prod.* **310**, 127431 (2021).
28. Spawn-Lee, S. A. et al. Comment on ‘Carbon intensity of corn ethanol in the United States: state of the science. *Environ. Res. Lett.* **16**, 118001 (2021).
29. Plevin, R. J., Gibbs, H. K., Duffy, J., Yui, S. & Yeh, S. *Agro-Ecological Zone Emission Factor (AEZ-EF) Model (v47): a Model of Greenhouse Gas Emissions from Land-use Change for Use with AEZ-base Economic Models*. GTAP technical paper No. 34 (Global Trade Analysis Center, Purdue University, Indiana, 2014).
30. Qin, Z., Dunn, J. B., Kwon, H., Mueller, S. & Wander, M. M. Influence of spatially dependent, modeled soil carbon emission factors on life-cycle greenhouse gas emissions of corn and cellulosic ethanol. *GCB Bioenergy* **8**, 1136–1149 (2016).
31. Searchinger, T. D., Beringer, T. & Strong, A. Does the world have low-carbon bioenergy potential from the dedicated use of land?. *Energy Policy* **110**, 434–446 (2017).
32. Sallustio, L., Harfouche, A. L., Salvati, L., Marchetti, M. & Corona, P. Evaluating the potential of marginal lands available for sustainable

cellulosic biofuel production in Italy. *Socio-Econ. Plan. Sci.* **82**, 101309 (2022).

33. Fargione, J., Hill, J., Tilman, D., Polasky, S. & Hawthorne, P. Land clearing and the biofuel carbon debt. *Science* **319**, 1235–1238 (2008).
34. Daioglou, V. et al. Greenhouse gas emission curves for advanced biofuel supply chains. *Nat. Clim. Change* **7**, 920–924 (2017).
35. Skevas, T., Swinton, S. M., Tanner, S., Sanford, G. & Thelen, K. D. Investment risk in bioenergy crops. *GCB Bioenergy* **8**, 1162–1177 (2016).
36. Miao, R. & Khanna, M. Effectiveness of the biomass crop assistance program: Roles of behavioral factors, credit Constraint, and program design. *Appl. Eco Perspect. Pol.* **39**, 584–608 (2017).
37. Valin, H. et al. *The Land Use Change Impact of Biofuels Consumed in the EU: Quantification of Area and Greenhouse Gas Impacts* (European Commission, 2015); [https://energy.ec.europa.eu/publications/land-use-change-impact-biofuels-consumed-eu\\_en](https://energy.ec.europa.eu/publications/land-use-change-impact-biofuels-consumed-eu_en)
38. Kwon, H. et al. Carbon calculator for land use and land management change from biofuels production (CCLUB). Argonne National Laboratory, ANL/ESD/12-5 Rev. 7. Available at <https://publications.anl.gov/anlpubs/2021/10/171711.pdf> (2021).
39. Copenhaver, K. & Mueller, S. Considering historical land use when estimating soil carbon stock changes of transitional croplands. *Sustainability* **16**, 734 (2024).
40. Iyer, G. et al. Measuring progress from nationally determined contributions to mid-century strategies. *Nat. Clim. Change* **7**, 871–874 (2017).
41. Wise, M., Muratori, M. & Kyle, P. Biojet fuels and emissions mitigation in aviation: an integrated assessment modeling analysis. *Transp. Res. Part D Transp. Environ.* **52**, 244–253 (2017).

## Acknowledgements

This work was funded by the DOE Center for Advanced Bioenergy and Bioproducts Innovation (U.S. Department of Energy, Office of Science, Biological and Environmental Research Program under Award Number DE-SC0018420). This work was partially supported by the Center for Bioenergy Innovation (CBI), U.S. Department of Energy, Office of Science, Biological and Environmental Research Program under Award Number ERKP886. Any opinions, findings, and conclusions or recommendations expressed in this publication are those of the author(s) and do not necessarily reflect the views of the U.S. Department of Energy.

## Author contributions

M.K. and W.W. designed the study. W.W. conducted the main modeling work and results analysis. M.K. and W.W. co-wrote the paper. E.B.-B., C.J.,

K.G., J.S.G., J.L.F., and E.H.D. provided essential data and methods for the analysis and valuable comments on the paper. All authors read and approved the final paper.

## Competing interests

The authors declare no competing interests.

## Additional information

**Supplementary information** The online version contains supplementary material available at <https://doi.org/10.1038/s43247-025-02913-x>.

**Correspondence** and requests for materials should be addressed to Madhu Khanna.

**Peer review information** *Communications Earth and Environment* thanks Gerd Angelkorte and Xin Zhao for their contribution to the peer review of this work. Primary Handling Editors: Pallav Purohit and Martina Grecequet. A peer review file is available.

**Reprints and permissions information** is available at <http://www.nature.com/reprints>

**Publisher's note** Springer Nature remains neutral with regard to jurisdictional claims in published maps and institutional affiliations.

**Open Access** This article is licensed under a Creative Commons Attribution 4.0 International License, which permits use, sharing, adaptation, distribution and reproduction in any medium or format, as long as you give appropriate credit to the original author(s) and the source, provide a link to the Creative Commons licence, and indicate if changes were made. The images or other third party material in this article are included in the article's Creative Commons licence, unless indicated otherwise in a credit line to the material. If material is not included in the article's Creative Commons licence and your intended use is not permitted by statutory regulation or exceeds the permitted use, you will need to obtain permission directly from the copyright holder. To view a copy of this licence, visit <http://creativecommons.org/licenses/by/4.0/>.

This is a U.S. Government work and not under copyright protection in the US; foreign copyright protection may apply 2025